Six-Port Reflectometer in WR15 Metallic Waveguide for Free-Space Sensing Applications

Kamel Haddadi, Christophe Loyez, Laurent Clavier, Denis Pomorski, Simon Lallemand

Six-Port Reflectometer in WR15 Metallic Waveguide for Free-Space Sensing Applications

[1]Kamel Haddadi, [1]Christophe Loyez, [1]Laurent Clavier, [2]Denis Pomorski and [3]Simon Lallemand

[1]Univ. Lille, CNRS, UMR 8520 - IEMN, F-59000 Lille, France
[2]Univ. Lille, CNRS, UMR 9189 – CRIStAL, F-59000 Lille, France
[3]Groupe Segula Technologies, Valenciennes, France
kamel.haddadi@iemn.univ-lille1.fr

***Abstract* — This work describes the design, fabrication and measurements of a six-port reflectometer in metallic waveguide technology for operation around 60 GHz. The system integration is based on WR15 building blocks. An in-situ linearization of the detectors associated to a vector calibration procedure is provided to determine the calibrated IQ components from the measured voltages. Near-field free-space distance measurements from contact to stand-off distance of two free-space wavelengths are shown to validate the technique proposed.**

***Index Terms* — Six-port, reflectometer, IQ demodulation, millimeter-wave, distance measurement,**

I. Introduction

The six-port technique has been introduced in the 1970s as a simple technique for measuring power and reflection coefficient in the microwave regime [1]. Since then, a variety of six-port systems have been exemplary demonstrated in metallic guide, substrate integrated waveguide (SIW), planar and monolithic forms [2]-[8]. Each technology presents own advantages and drawbacks in terms of circuit size, power consumption, immunity to temperature/hygrometry variations, fabrication facility, system integration, measurement performance and cost [8]. Therefore, the choice of the technology is mainly driven by the requirements of the targeted application.

This work presents a fully WR15 metallic waveguide six-port reflectometer operating at 60 GHz for near-field sensing applications, i.e. near-field high precision distance measurement. Unlike planar technologies systems, waveguides are highly shielded to provide isolation between nearby signals. As they rely on air as a dielectric, the technology reduces the need for consistency in the dielectric material and presents better immunity to environmental variations. Furthermore, the building blocks of the six-port circuit can be easily connected each other as they are inherently matched. As the size is directly related to the operation wavelength, millimeter-wave frequency operation is preferred to reduce the circuit size.

II. Six-Port IQ demodulator

This section describes the design, fabrication and test of the six-port IQ demodulator. The proposed architecture and picture of the fabricated system are given in Fig. 1.

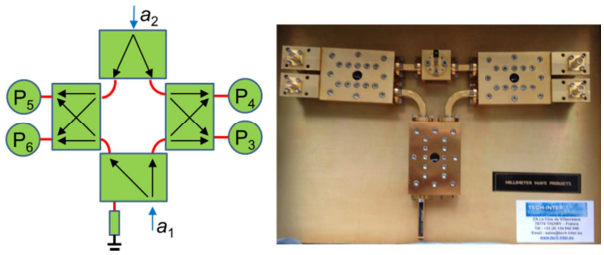

Fig. 1. (a) Structure of the six-port IQ demodulator. (b) Photograph of the WR15 waveguide six-port IQ demodulator.

The circuit is implemented using three 90° hybrids with 20 dB isolation and 6 % bandwidth around 60 GHz, a four port hybrid tee with one arm connected to a match termination for basic power splitting and four power detectors with typical video sensitivity of 500 mV/mW and tangential sensitivity of -50 dBm. Interconnecting bends and twists are used for system integration. The reference millimeter-wave signal a_1 [fig. 1(a)] can be provided by a miniature high stability phase-locked source Mi-WAVE™ 957 (P_{LO} = 11 dBm) or a frequency synthetizer Keysight™ E8257D.

The first step concerns the linearization of the electrical response of the power detectors to correct deviation from quadratic response. For this experiment, the RF port (signal a_2) of the six-port demodulator is connected to a match termination to make the electrical response depending only of the LO source signal a_1. We present in Fig. 2 the detected voltages V_1 to V_4 measured for a source power varying from 10 µW to 10 mW at 60 GHz.

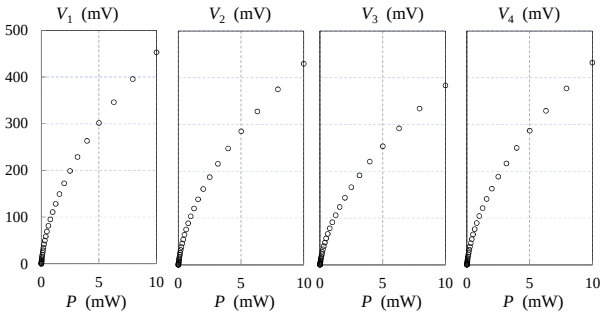

Fig. 2. Detected voltages as a function of the input millimeter-wave LO power – F = 60 GHz.

From Fig. 2, the linearity is degraded by distorsions. The linearization procedure consists to interpolate the measured data using a polynomial function. In this study, a 5th order polynomial is used. As an example, the interpolation model for the voltage V_1 is given by

$$P_1 \text{ (mW)} = -1.43\times10^{-13}\, V_1^5 + 1.66\times10^{-10}\, V_1^4 - 8.04\times10^{-8}\, V_1^3 + 5.98\times10^{-5}\, V_1^2 + 4.02\times10^{-3}\, V_1 + 1.36\times10^{-2}.$$

The next step consists of verifying the performance in mixing mode. In this configuration, the millimeter-wave signal a_2 with amplitude A_{RF} is combined with the signal a_1 with amplitude A_{LO}. The theoretical powers P_3 to P_6 are given by

$$P_3 = |0.5(a_2 + a_1)|^2 \quad (1)$$

$$P_4 = |0.5(a_2 - ja_1)|^2 \quad (2)$$

$$P_5 = |0.5(a_2 - a_1)|^2 \quad (3)$$

$$P_6 = |0.5(a_2 + ja_1)|^2 \quad (4)$$

The 60 GHz LO and RF input signals are both obtained by the synthesizer using a power splitter. The source power is set to 11 dBm. The RF signal amplitude A_{RF} and relative phase-shift $\Delta\Phi$ are respectively adjusted with precise WR15 waveguide variable attenuator (MI-WAVE 510V/385) and phase-shifter (MI-WAVE 528V/385) as shown in Fig. 3. The IQ components are defined as

$$I = A_{RF}\cos(\Delta\Phi) \sim P_3 - P_5 \quad (5)$$

$$Q = A_{RF}\sin(\Delta\Phi) \sim P_6 - P_4 \quad (6)$$

A spatial (related to the spatial phase-shift $\Delta\Phi$) Fourier analysis is considered to correct the general forms given by (5) and (6) into the models (7) and (8) that encompasses mismatching and non-linear effects [9].

$$P_3 - P_5 = y_0 + y_1 I + y_2 Q + y_3 I^2 + y_4 Q^2 + y_5(I^2 - 3IQ^2) + y_5(Q^2 - 3I^2 Q) \quad (7)$$

$$P_6 - P_4 = y'_0 + y'_1 I + y'_2 Q + y'_3 I^2 + y'_4 Q^2 + y'_5(I^2 - 3IQ^2) + y'_6(Q^2 - 3I^2 Q) \quad (8)$$

These equations rely the powers to polynomial combinations of I and Q through eight real calibration constants y_i and y'_i. More information about the model construction is given in [9].

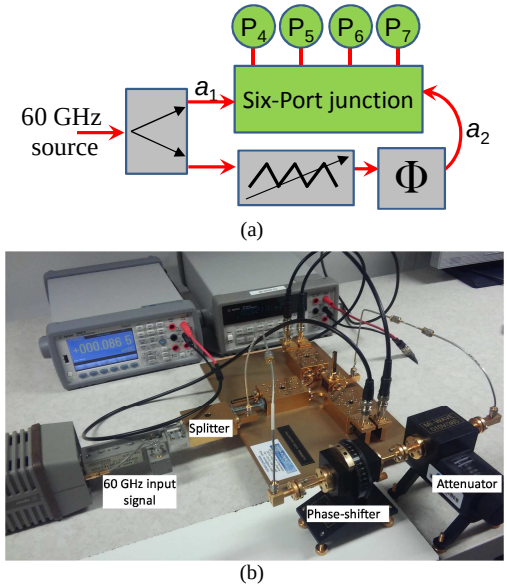

Fig. 3. Experimental test bench arrangement for IQ measurements.

The calibration coefficients y_i and y'_i are determined by fitting the measured powers to the models (7) and (8). For comparison purposes, the calibration constants are determined for the 1st ($y_3 = y_4$ and $y_5 = y_6 = y_7 = 0$), the 2nd ($y_6 = y_7 = 0$) and the 3rd orders. Table I reports the parameters obtained for $P_3 - P_5$. The 3D fitting according to the 3rd order model is also illustrated in Fig. 4. These results show that the spatial non-linearity effect has relatively low impact. However, metrological applications that require a high degree of accuracy can benefit from a 3rd order model that achieves a determination coefficient of nearly 1 computed on 259 points. Equivalent result has been found for $P_6 - P_4$. The calibration has been also validated in the frequency band 55-75 GHz.

TABLE I. CALIBRATION COEFFICIENTS ESTABLISHED FOR $P_3 - P_5$ – F=60 GHz.

Coefficient	Parameter	Order 1	Order 2	Order 3
Y_0	1	-0.2457	-0.2457	-0.2457
y_1	I	0.6575	0.6592	0.6593
y_2	Q	-1.1466	-1.1466	-1.1466
y_3	I^2	-0.0102	-0.0504	-0.0504
y_4	Q^2		0.0321	0.0321
y_5	IQ		-0.0152	-0.0152
y_6	I^3-3 I Q^2	—	—	-0.0001
y_7	Q^3-3 I^2 Q			-0.0128
r^2		*99.80%*	*99.88%*	*99.89%*

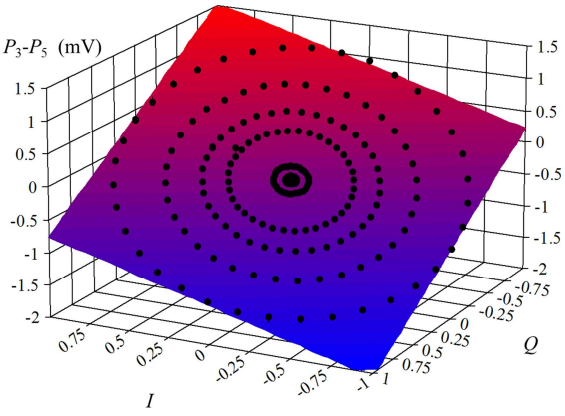

Fig. 4. IQ demodulation at 60 GHz: 3D complex interpolation – F=60 GHz. (● Measured data).

II. Distance Sensing Applications

A distance measurement sensor based on the six-port demodulator associated to WR15 power divider, circulator and horn antenna is given in Fig. 5. The antenna with vertical polarization has been tested with stand-off *d* from contact to 10 mm to a metallic target. For example, detected voltage V_1 as a function of *d* shows the spread propagation losses that increase with *d*. Furthermore, resonances are related to wave recombination between the reflected wave by that target, the guided reflected wave at the antenna input (mismatch) and the free-space source match term (reflection of the received wave by the antenna). A dedicated free-space calibration method that takes into account these two effects can be implemented to derive the distance as a function of the measured voltages [10]. Complementary results will be shown in the last version of the paper.

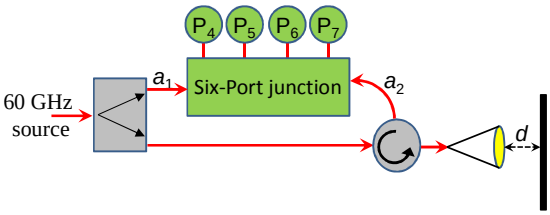

(a)

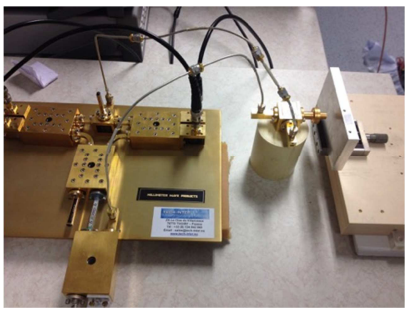

(b)

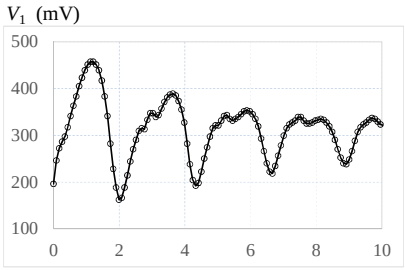

(c)

Fig. 5. Free-space distance measurement – F = 60 GHz. (a) and (b) Experimental test bench. (c) Detected voltage V_1 as a function of the stand-off *d*.

V. Conclusion

A 60 GHz six-port IQ demodulator in WR15 guide technology has been designed and tested. On this basis, a free-space six-port reflectometer has been described for close distance measurement in the cm range. Preliminary experiments show propagation of spherical waves combined with free-space stationary waves. Future work will provide all necessary calibration procedure for accurate extraction of distance and precision analysis.

References

[1] G. Engen and C. Hoer, "Application of an arbitrary 6-port junction to power-measurement problems," *IEEE Trans. Instrum. Meas.*, vol. 21, no. 4, pp. 470–474, Nov. 1972.

[2] J. Li, R. G. Bosisio, and K. Wu, "A collision avoidance radar using six-port phase/frequency discriminator," *Proc. IEEE MTT-S Dig.*, pp. 1553–1555, May 1994.

[3] J. Osth, A. Serban, O. Owais, M. Karlsson, S. Gong, J. Haartsen, and P. Karlsson, "Six-port gigabit demodulator", *IEEE Trans. Microw. Theory Tech.*, vol. 59, no. 1, pp. 125–131, January 2011.

[4] A. Koelpin, G. Vinci, B. Laemmle, D. Kissinger and R. Weigel, "The six-port in modern society," *IEEE Microw. Mag.*, vol. 11, no. 7, pp. 35–43, Dec. 2010.

[5] A. Moscoso-Mártir, J.M. Ávila-Ruiz, E. Durán-Valdeiglesias, L. Moreno-Pozas, I. Molina-Fernández, A. Ortega-Moñux and J. de-Oliva-Rubio, "Butler matrix based six-port passive junction," *IEEE WiSNet*, pp.7–9, Jan. 2014.

[6] S. O. Tatu, A. Serban, M. Helaoui and A. Koelpin, "Multiport technology: the new rise of an old concept," *IEEE Microw. Mag.*, vol. 15, no. 7, pp. 34–44, Nov. 2014.

[7] B. Laemmle, G. Vinci, L. Maurer, R. Weigel, and A. Koelpin, "A 77-GHz SiGe integrated six-port receiver front-end for angle-of-arrival detection," *IEEE J. Solid-State Circuits*, vol. 47, no. 9, pp. 1966–1973, Sept. 2012.

[8] A. Koelpin, F. Lurz, S. Linz, S. Mann, C. Will and S. Lindner, "Six-port based interferometry for precise radar and sensing applications", *Sensors*, vol. 16, no. 1556, pp. 1–26, Sept. 2016.

[9] K. Haddadi and T. Lasri, "Formulation for complete and accurate calibration of six-port reflectometers", *IEEE Trans. Microw. Theory Tech.*, vol. 60, no. 3, pp. 574–581, March 2012.

[10] K. Haddadi, MM.Wang, O. Benzaim, D. Glay, and T. Lasri, "Contactless microwave technique based on a spread-loss model for dielectric materials characterization", *IEEE Microw. Wireless Compon. Lett.*, vol. 19, no. 1, pp. 33–35, Jan. 2009.